https://doi.org/10.5194/angeo-2019-124
Preprint. Discussion started: 18 September 2019

Annales Geophysicae Discussions

Localized TEC enhancements in the Southern Hemisphere

Ilya K. Edemskiy[1]

[1]Institute of Atmospheric Physics, Czech Academy of Sciences, Prague, Czech Republic

Correspondence to: Ilya K. Edemskiy (edi@ufa.cas.cz)

Abstract. The paper is dedicated to investigation of localized TEC (total electron content) enhancements (LTEs), particularly of LTE series, detected in the Southern Hemisphere using global ionospheric maps for different solar activity years (2014, 2015, 2018). It is shown that LTE intensity varies in dependence on solar flux and does not directly depend on interplanetary magnetic field orientation. The enhancements occur in a subsolar region and could be observed during a continuous series of days. The highest LTE occurrence rate is observed during period of local winter (April-September) for all analyzed years. The longest observed LTE series was detected during 2014 and lasted 80 days or 120 days if we exclude 2 daily gaps.

1 Introduction

The Southern Hemisphere (SH) ionosphere has not been investigated so broadly as the one of Northern Hemisphere (NH). Historically, most of the geophysical observations and measurements have been made to the north of the equator. Even now, having lots of observatories all around the globe, we have a lack of ground-based observations for a larger part of the Southern Hemisphere since it is mostly occupied by ocean. Satellite measurements allow us to investigate ionosphere over oceans but due to its high variability and the movement of satellites it is very difficult to observe the same region in the same conditions.

The Southern Hemisphere contains at least two large anomalous regions: South Atlantic Magnetic Anomaly and Weddell Sea Anomaly. The latter consists in the modulation of TEC's diurnal oscillations by the solar-modulated seasonal oscillations, which produces a diurnal anomaly in the vicinity of the Weddell Sea during Southern Hemisphere summer (October to March) (Lean et al., 2016). So called nighttime winter anomaly (NWA) was shown to occur during low solar activity period in Asian longitudinal sector of SH (Jakowski et al., 2015). In general the winter anomaly in SH does not manifest itself with the same intensity as that in NH (Yasyukevich et al., 2018). Globally ionosphere dynamics in the both hemispheres is different.

The most widely used and generally accepted the International Reference Ionosphere (IRI) empirical model (e.g., Bilitza, 2018) does not predict some features of the SH ionosphere sufficiently. Karia et al. (2019) analyzing predictions of IRI-2016 showed that the model does reproduce the observed NWA effect. Comparing TEC measurements and results of IRI-PLAS, Alcay and Oztan (2019) found that in SH the model generally overestimates the GPS-TEC measured at stand-alone stations with the maximum difference about 15 TECU. Karpachev and Klimenko (2018) proposed a new model reproducing the

https://doi.org/10.5194/angeo-2019-124
Preprint. Discussion started: 18 September 2019

Annales Geophysicae Discussions

structure of the high-latitude ionosphere more accurately than IRI-2016 and noted that inaccuracies of IRI in that region are connected with inaccuracy of ground-based sounding data, which varies during a day. However, none of these models predict the occurrence of the LTE phenomenon.

During analysis of ionosphere response to a geomagnetic storm of 15 August 2015, a curious structure was detected in global ionospheric maps (GIMs), which we call localized TEC enhancement or LTE (Edemskiy et al., 2018). The enhancement was detected in the Southern Hemisphere and lasted for several hours. Assuming the phenomenon to be rare, we developed a detection algorithm, which allowed us to find about 30 similar events in the Southern Hemisphere during 2010-2016 and to suggest direct connection of their occurrence rate with solar activity. Unfortunately the algorithm had disadvantages: fixed detection threshold and comparison with a weekly median TEC value. The first assumption did not allow us to detect relatively weak but existing LTEs, the second one excluded from the consideration possible series of such disturbances.

The present article is an attempt to detect more LTEs during different solar activity periods and to investigate them more carefully trying to understand mechanisms of their generation. Section 2 describes data and methods, section 3 presents results, section 4 deals with discussion and possible mechanism, and section five summarizes main results.

2 Data and methods

The localized TEC enhancement is a positive disturbance of ionosphere. To distinguish it from other large-scale disturbances of electron concentration we introduce detection criteria:

1. Spatial limitation and clear borders. An enhancement should not be wider than 40° and 120° in latitude and longitude, respectively. Gradients at an LTE edges should be high enough to make LTE borders possible to distinguish. If an enhancement occupies relatively wide area, stretched in any direction (usually along a geomagnetic parallel) for more than 120° or has no significant variations of intensity we do not take such disturbance into consideration.

2. Location in the mid- or subpolar-latitude dayside ionosphere of Southern Hemisphere (30-70°S of geomagnetic latitude). We search LTEs only in the Southern Hemisphere, because Edemskiy et al. (2018) detected LTEs only at SH. A disturbance should follow the Sun having the maximal intensity no latter than 1-2 hours after local noon (in a period 12-14 LT as observed by Edemskiy et al., 2017). All the others localized enhancements, observed at local night, morning or evening are not considered.

According to these criteria we detect LTEs in global ionospheric maps.

Currently, global ionospheric maps are provided by several scientific groups: CODE (codg), ESA (esag), JPL (jplg), UPC (upcg), Whuan university (whug), Chinese Academy of Sciences (CAS - casg). IGS service also provides maps (igsg) created as a combination of maps from CODE, UPS, ESA and JPL. The spatial resolution is 2.5°x5° in latitude and longitude, respectively, and temporal one is 2 h (1 h for CODE maps since 2015). Maps are calculated from slant (sTEC) values measured at 200-350 (depending on the data availability and the used method) GNSS receivers all around the world with application of some interpolation method. Global ionospheric maps from all the above mentioned groups are freely available at CDDIS server (ftp://cddis.gsfc.nasa.gov/gps/products/ionex). According to Roma-Dollase et al. (2018) CODE

https://doi.org/10.5194/angeo-2019-124
Preprint. Discussion started: 18 September 2019

Annales Geophysicae Discussions

and CAS maps have the lowest relative errors in the South Atlantic and Indian Ocean regions. Taking into account the high temporal resolution of CODE maps and more clear information about the used data in the headers of these maps, we use CODE GIMs in the present paper.

To confirm an LTE presence we use measurements from SWARM and COSMIC satellite missions. The SWARM mission was launched by ESA at the end of 2013. It is mainly aimed to investigation of Earth's magnetic field. The mission includes three satellites at polar orbits of about 500 km (460 km for Alpha and Charlie, and 530 km for Bravo). The data are available via browser-based application (https://vires.services/) or via API tool (https://github.com/ESA-VirES/VirES-Python-Client). In the present paper in-situ measurements of electron density are used.

The project COSMIC (Constellation Observing System for Meteorology Ionosphere & Climate) provide measurements of upper atmosphere and ionosphere parameters. In the present paper we use TEC profiles obtained via radio occultation (RO) receiving of GPS signals. To distinguish this data from the standard ground-based TEC measurements, we use abbreviation SS TEC (satellite-to-satellite TEC). COSMIC data is freely provided as NetCDF files (https://cdaac-www.cosmic.ucar.edu/).

We analyze mainly the occurrence rate of LTE and its dependence on space weather. Quantitative analysis of LTEs generally consists of definition of maximal TEC value over the investigation region and calculation of its relation to mean TEC value over the region. Analysis of the dependence of these parameters on near space conditions was made during the investigation. LTE shapes vary widely and are quite difficult for formalization.

To analyze connection of the observed features of ionospheric dynamics with geomagnetic field we use SuperDARN altitude adjusted corrected geomagnetic coordinates (AACGM) (Shepherd, 2014) as a Python module developed by Angeline Burrell (https://github.com/aburrell/aacgmv2). To create maps in geomagnetic coordinates we place each TEC cell from GIM map at the corresponding magnetic latitude and longitude calculated with AACGM for an altitude of 100 km.

Files of GIMs in IONEX format were treated with the python package GNSS-LAB created by Ilya Zhivetiev (https://pypi.org/project/gnss-tec/). Processing and presentation of data were made with Python libraries Numpy (https://numpy.org) and Pandas (https://pandas.pydata.org/). Geomagnetic indices and other parameters of near space were taken from OMNI database (https://omniweb.gsfc.nasa.gov).

3 Results

An example of a clearly observed LTE was detected at April 5, 2014 (Fig. 1). The disturbance reached the highest intensity in a period 10-12 UT when TEC values in a center of the disturbance exceeded 78 TECU. This value is comparable to equatorial TEC values. The highest values were detected in a latitudinal region 45-70°S. At the same time, TEC values of the entire region (30-70°S, 0-90°E) were enhanced.

It is possible to distinguish two parts in presented LTE: midlatitudinal (MLTE) and subpolar (SLTE). The LTE of April 5 has strong subpolar part and weaker but still pronounced midlatitudinal one. As it will be shown later, such a strong SLTE is not typical and in some cases it is not detected at all.

https://doi.org/10.5194/angeo-2019-124
Preprint. Discussion started: 18 September 2019

Annales Geophysicae Discussions

During its development the LTE changes latitudinal position in a range 30-80°S and varies along geomagnetic parallels within 35-70°S range of geomagnetic latitudes (red lines in Fig. 1A). Phases of the development during April 5 are shown in geomagnetic coordinates (AACGM) in panels B-K in Fig. 1. As it could be seen from the figure, the LTE exists during the entire day and changes its intensity unevenly. The less intensive MLTE part persists for a longer time and has lower magnitude than the brighter SLTE. Both parts are confined in their own ranges of geomagnetic latitudes: 30-50°S and 50-65°S, respectively. During the whole period shown their positions keep approximately the subsolar point (local noon).

It is necessary to say that the LTEs are detected most clearly over Atlantic and Indian oceans, where amount of GNSS stations is insufficient. White squares in Fig. 1 mark location of the receivers providing CODE with data for TEC maps. Only a few are located in ocean and the only is in 30-60°S latitudes of Indian Ocean (Kerguelen Islands, KERG). Therefore LTE detection has to be confirmed by other observations.

In-situ measurement of electron concentration Ne from SWARM satellites allow us to check validity of TEC distribution presented by GIM. Left panel of figure 2 presents Ne values, observed during 8-14 UT at April 5, 2014. Each track is marked by a colored dot corresponding to satellite: Alpha (red), Bravo (blue) and Charlie (cyan); digits of the corresponding color marks the satellite position at the the beginning and the end of the track in a format HHMM (hours and minutes). All the satellites were moving from equator to pole.

The area of extremely high concentration of electrons is clearly observed in data from all the three satellites. Blank areas in measurements from Alpha and Charlie during 11:30-13:30 mark the zone of concentrations exceeding color axis limitation. Temporal differences between passages of the satellites allow us to observe the dynamics of the LTE. The most intensive part is shown by Alpha's measurements. Charlie is ahead of Alpha by about 15 minutes and 2.5° of longitude and its measurements in general show lower concentration especially for a period 8-12 UT. Most probably such a difference is caused by movement of the enhancement: according to the GIM LTE is located in subsolar region and follows the Sun. Bravo is about 30 min and 12° behind Alpha and its measurements shows significantly lower concentration than the other satellites. It could point not only to the disturbance displacement but also to its distribution with altitude, since the orbit of Bravo is 70 km higher than those of Alpha and Charlie.

The distribution of electron concentration with altitude can be analyzed using radio occultation measurements by COSMIC satellites. Profiles of SS TEC during April 5 are presented in the right panel of Fig. 2. Each SS TEC value in a profile is obtained from a bent satellite-to-satellite signal and is attributed to a tangent point of the signal (Rocken et al., 2000). Projections of the tangent points during each profile measurement are shown in left panel of Fig. 2 with the same color as the profile. Cross marks on the trajectories and nearby digits indicate location and time of the lowest altitude measurement (last measured value before GPS satellite occultation). Blue dashed line (Fig. 2, right) presents a profile measured at 10:12 UT at October 19, 2014 when there was no LTE observed in GIM. It is quite clear that the detected disturbance was propagating according to solar motion and had the highest electron concentration in F region at about 11 UT. Profiles also show that electron concentration at an altitude 460 km could be 1.5-2 times higher that at 530 km, which is in a correspondence with SWARM measurements.

https://doi.org/10.5194/angeo-2019-124
Preprint. Discussion started: 18 September 2019

LTEs similar to the one detected on April 5 could be observed during several days in a row. In the particular case of April 2014, LTEs southward of Africa were detected since March 18 till April 11. TEC maps at 10:00 UT for April 1-9, 2014 are presented at the left side of Fig. 3. The geomagnetic conditions during this period were slightly disturbed: maximal value of Kp was 4 (April 7), and minimal Dst value was about -25 nT (April 7-8). The intensity and the shape of the presented LTEs vary but at the same time of day all of them occupy the same region. Intensities of MLTE and SLTE vary independently. SLTE is more intense only on April 5. Mostly its intensity is either close to that of MLTE (April 1, 3, 4, 7, 9) or weaker (April 2, 6 and 8).

In a similar way LTE series were observed during other investigated years of relatively high (2015) and low (2018) solar activity (figure 3, middle and right). Intensity of the observed LTEs varies according to global electron content, which depends on solar activity (e.g., Afraimovich et al., 2008). Disturbances of 2015 still have two different zones of LTEs, while all the presented LTEs of 2018 apparently are of MLTE type (see April 6 in Fig. 3, left). Geomagnetic activity during the presented days was from moderate to low and there was no clear correlation between indices (Kp, Dst, etc.) and a form or intensity of the disturbances.

The series of LTE are most often observed in autumn and at the beginning of winter (since March till June-July), as Fig. 4 shows. Each inner sector in Fig. 4 represents a months and its color depicts the season: summer (orange), autumn (red), winter (blue) and spring (green). Percentage shows the part of the month occupied by series of LTEs. For example, all the cases from Fig. 3 give 9-day series. If such a series was the only series during the month (30 days) the percentage will be 9/30 = 30%. Zero percentage does not mean absence of an LTE during a given period but only the absence of a LTE series.

As it is seen from Fig. 4, the absolute maximum of LTE series occurrence is observed in spring-summer period with the highest values during April-June. In late autumn and in winter no LTE series were usually observed. The most interesting series here is one, which lasted 80 days since May to July of 2014 (Fig. 4, left). It is quite clear that only short gaps (one day in both cases) separate this series from two others in spring and probably the entire period late March-July should be considered to include one long series. Such a long series occupying one third of a year definitely points to some regular process.

For the other years the same season contains majority of the LTE series, but divided with more frequent and wider gaps. It is interesting to see that during a year of low solar activity (2018) we detect more series than during a moderately active one (2015).

Due to large variety of spatial forms and intensity distributions of LTEs (Fig. 2) it is not easy to select a key parameter for an analysis over three years. We simplified the task by analyzing variations of maximal TEC value observed at 10 UT in a region 30°W-60°E, 30-60°S. It was found that during active years (2014-2015) maximal value quite clearly depends on F10.7 index (fig 5, top left). It was not a surprise since maximal value directly depends on the entire amount of electrons in ionosphere, which is driven by solar radiation. Taking this into account and supposing that not the whole region is usually occupied by the disturbance we analyzed, the ratio between maximal value and mean TEC over the given region. The distribution of this ratio vs IMF intensity is shown in right panels of Fig. 5. The most probable value of the ratio is about 1.4-

https://doi.org/10.5194/angeo-2019-124
Preprint. Discussion started: 18 September 2019


Annales Geophysicae Discussions

1.6 for 2014-2015 and 1.4-1.7 for 2018. We found that the ratio does not depend directly on space weather parameters, but its upper limit increases with intensity of interplanetary magnetic field (IMF) (Fig. 5, right).

4 Discussion

Being observed separately LTEs were previously supposed to be a relatively rare phenomenon produced by some specific condition of near space and the detection algorithm was based on this concept (Edemskiy et al., 2018). Mainly the detection was based on a comparison of near-days maps which does not allow detection of a disturbance during a series of them. Here we showed that LTEs occur more often and it is possible to observe a sequence of such disturbances during a relatively long period when geomagnetic and solar conditions could vary significantly. Analysis of LTE occurrence connection with parameters of near space did not reveal any pronounced dependence except the one between maximal TEC value in the region and solar flux intensity (Fig. 5, left). It shows a rise of disturbance intensity with global (or background) electron concentration, which dependence on F10.7 index is known (e.g., Astafyeva et al., 2008). Figure 5 (right panels) demonstrates essentially no dependence of occurrence frequency of LTE and of ratio of maximal to mean regional TEC on IMF. The previous suggestion (Edemskiy et al., 2018) of LTE occurrence only during disturbed conditions and especially with the observed negative Bz appears not to be entirely correct.

The height structure of the observed enhancements is not really clear. Cherniak et al. (2012) showed that daytime TEC in middle latitudes of Southern Hemisphere is by 30-40% formed in the plasmasphere. According to the maps of ionospheric ($h < 700$ km) and plasmaspheric (700 km $< h <$ 20000 km) content they presented, the plasmasphere contained more large-scale long-term disturbances than the ionosphere during all the four seasons of 2009. SWARM data confirmed presence of an LTE with in-situ measurements at the both altitudes of the satellites orbits and COSMIC measurements do not show any specific changes in shape of ionospheric profiles: SS TEC changes at different heights are similar. This is a good argument to believe that LTEs are predominantly located in the F2 region. At the same time, there were no SS TEC profiles available for the areas of the disturbances highest intensity (neither SLTE nor MLTE). It also should be noted that MLTE was not observed in SWARM data as clearly as SLTE and that could mean that effective altitudes of MLTE and SLTE might be different.

The presented seasonal distribution of LTEs shows the highest probability of their detection in the period of local autumn-winter independently of solar activity. Due to the solar zenith angle the Sun affects the ionosphere more intensively at local summer (December) producing more electrons than at local winter (July). For example, Gowtam and Tulasi Ram (2017) using COSMIC RO data showed the presence of this seasonal difference for altitudes within 300-700 km. The data presented above (Fig. 4) reveal higher occurrence rate of LTE during a period of higher solar zenith angles (local winter and autumn).

Similar seasonal asymmetry is known for the phenomenon of Winter Anomaly. It has been investigated mostly with NmF2 measurements in the Northern Hemisphere (e.g., Rishbeth et al., 2005). Some papers are dedicated to its global manifestation (e.g., Mendillo et al., 2005). In the Southern Hemisphere the anomaly is much less pronounced and the region of its observation is mostly located in the southern part of Indian Ocean (Yasyukevich et. al., 2018). Using GIM data (JPL, 1998-2015) and satellite measurements (2001-2015) those authors showed dependence of the anomaly intensity on solar activity

https://doi.org/10.5194/angeo-2019-124
Preprint. Discussion started: 18 September 2019

and claimed its absence during low activity periods. Their results revealed that winter anomaly in the Southern Hemisphere could be observed only during periods of high solar activity: in NmF2 it is observed with F10.7 > 90 SFU and in TEC with F10.7 > 170 SFU. Our results show LTE presence during all three years, even during 2018 when F10.7 annual mean was about 70 SFU and the highest F10.7 with an LTE detected was 85 SFU (Fig. 5). Therefore the mechanism of an LTE generation probably differs from that of Winter Anomaly.

Being observed dynamically LTEs show development along geomagnetic parallels within 30-70°S of geomagnetic latitude, approximately in boundaries of magnetic shells L = 2-4 (Fig. 1 B-K), and could be observed permanently for several days with slight changes of their form and intensity. Anderson et al. (2014) detected hotspot of energetic electron precipitation E > 300 keV at SH at geomagnetic latitudes 55–72oS (much less pronounced at NH) and geographic longitudes 150oW–60oE. However, this result is based on nighttime observations, i.e. predominantly autumn-winter observations, when almost no LTEs have been detected. Using POES data for analysis of South Atlantic Anomaly, Domingos et al. (2017) found a plume of particle flux located within L=2.5-3 in South Atlantic. The position of the plume was in a good correlation with a typical LTE position. However, the plume was observed in December when occurrence rate is minimal (Fig. 4). Moreover, for the LTE analyzed in detail by Edemskiy et al. (2018) it was shown that particle precipitations is not responsible for that LTE. So most probably LTEs are not directly connected with the increased fluxes.

Statistically the ionosphere over the western part of Indian Ocean has enhanced electron concentration during equinox periods. Jee et al. (2009) investigating TOPEX data over 1992-2005 showed that during March-April noontime TEC values are significantly increased over the southern part of Africa and its Indian Ocean shore. Similar increment with lower intensity could be seen during September-October. At summertime it is still possible to observe this enhancement with much less intensity. In winter the region of enhanced TEC depends on solar activity: during high activity period no enhancement is observed. During low activity the Equatorial Anomaly area is shown to wider, reaching 30ºS over Africa and TEC values at south of Africa are increased as well. Our results show higher probability of wintertime LTE detection during lower activity years. Analyzing GIMs for 1998-2015 Lean et al. (2016) found typically enhanced TEC over the region during 10-16UT and according to data for 2000-2002 the highest values during March-May.

Investigating GRACE and CHAMP electron density measurements over a period 2003-2007, Lee et al. (2011) also showed presence of enhanced electron concentration formation over western part of Indian Ocean. This formation is clearer in a presented difference between IRI (2001 and 2007) data and satellite measurements. Such a clear difference shows that the enhancement phenomenon in the region is not taken into account in the models.

5 Discussion

Localized TEC enhancement is a relatively frequent phenomenon in the Southern Hemisphere, which could be observed during several months under different ionospheric conditions. The highest probability to observe an LTE series is in spring-summer period (April-June), whereas it is almost zero in November-February (summer). An LTE develops in latitudinal region corresponding to L = 2-4 geomagnetic shells and its intensity clearly depends on solar activity. The most probable

https://doi.org/10.5194/angeo-2019-124
Preprint. Discussion started: 18 September 2019

LTE intensity is essentially independent of IMF intensity and it is 1.4-1.6 times higher than the mean TEC in the region between Africa and Antarctica. No clear dependence between orientation of IMF and LTEs' parameters was observed. Formation of LTE varies with solar activity and usually do not contain pronounced southern plume during low solar activity. The phenomenon is not predicted by the IRI model.

Acknowledgements

The author is grateful to Jan Laštovička for the idea of the investigation, for fruitful discussions and corrections of the text. Author thanks Martin Pačes for his kind help with obtaining SWARM data and Nikolay Zolotarev for his help with COSMIC data treatment. Thanks to all the data centers, which provided data: NASA's Crustal Dynamics Data Information System (CDDIS), CODE scientific group, SWARM and COSMIC mission staff.

References

Afonin, V.V., Benkova, N.P., Besprozvannaya, A.S., Shchuka, T.I., Zikrach, E.K. and Shestakova, L.V.: The ionospheric trough dynamics in the northern and southern Hemispheres: the longitudinal and IMF effect, J. Atmos. Terr. Phys., 57, 1057-1062, https://doi.org/10.1016/0021-9169(95)96865-T, 1995.

Afraimovich, E. L., Astafyeva, E. I., Oinats, A. V., Yasukevich, Yu. V., and Zhivetiev, I. V.: Global electron content: a new conception to track solar activity, Ann. Geophys., 26, 335-344, https://doi.org/10.5194/angeo-26-335-2008, 2008.

Alcay, S. and Oztan, G.: Analysis of global TEC prediction performance of IRI-PLAS model, Adv. Space Res., 63, 10, 3200-3212, https://doi.org/10.1016/j.asr.2019.02.002, 2019.

Andersson, M. E., Verronen, P. T., Rodger, C. J., Clilverd, M. A., and Wang, S.: Longitudinal hotspots in the mesospheric OH variations due to energetic electron precipitation, Atmos. Chem. Phys., 14, 1095–1105, https://doi.org/10.5194/acp-14-1095-2014, 2014.

Astafyeva, E.I., Afraimovich, E.L., Oinats, A.V., Yasukevich, Yu.V., and Zhivetiev, I.V.: Dynamics of global electron content in 1998–2005 derived from global GPS data and IRI modeling, Adv. Space Res., 42, 4, 763-769, https://doi.org/10.1016/j.asr.2007.11.007, 2008.

Bilitza, D.: IRI the International Standard for the Ionosphere, Adv. Radio Sci., 16, 1-11, doi: 10.5194/ars-16-1-2018, 2018.

Chen, C.H., Huba, J.D., Saito, A., Lin, C.H., and Liu J.Y.: Theoretical study of the ionospheric Weddell SeaAnomaly using SAMI2, J. Geophys. Res.,116, A04305, doi:10.1029/2010JA015573, 2011.

Domingos, J., Jault, D., Pais, M.A., and Mandea, M.: The South Atlantic Anomaly throughout the solar cycle, Earth Plan. Sci. Lett., 473, 154-163, https://doi.org/10.1016/j.epsl.2017.06.004, 2017.

Edemskiy, I., Lastovicka, J., Buresova, D., Habarulema, J. B., and Nepomnyashchikh, I.: Unexpected Southern Hemisphere ionospheric response to geomagnetic storm of 15 August 2015, Ann. Geophys., 36, 71-79, https://doi.org/10.5194/angeo-36-71-2018, 2018.

https://doi.org/10.5194/angeo-2019-124
Preprint. Discussion started: 18 September 2019

Gowtam, S.V., and Tulasi Ram, S.: Ionospheric winter anomaly and annual anomaly observed from Formosat-3/COSMIC Radio Occultation observations during the ascending phase of solar cycle 24. Adv. Space Res., 60, 8, 1585-1593, http://dx.doi.org/10.1016/j.asr.2017.03.017, 2017.

He, M., Liu, L., Wan, W., and Zhao, B.: A study on the nighttime midlatitude ionospheric trough,J. Geophys.Res.,116, A05315, doi:10.1029/2010JA016252, 2011.

Horvath, I. and Lovell, B.C.: Investigating the relationships among the South Atlantic Magnetic Anomaly, southern nighttime midlatitude trough, and nighttime Weddell Sea Anomaly during southern summer, J. Geophys. Res., 114, A02306, doi:10.1029/2008JA013719, 2009.

Jakowski, N., Hoque, M.M., Kriegel, M., and Patidar, V.: The persistence of the NWA effect during the low solar activity period 2007–2009, J. Geophys. Res. Space Phys., 120, 9148–9160, doi:10.1002/2015JA021600, 2015.

Jee, G., Burns, A.G., Kim, Y.-H., and Wang, W.: Seasonal and solar activity variations of the Weddell Sea Anomaly observed in the TOPEX total electron content measurements, J. Geophys. Res., 114, A04307, doi:10.1029/2008JA013801, 2009.

Karpachev, A.T., and Klimenko, M.V.: Satellite Model of FoF2 in the High-Latitude Winter Ionosphere of the Northern and Southern Hemispheres, 2nd URSI Atlantic Radio Science Meeting (AT-RASC), Meloneras, 2018, pp. 1-4. doi: 10.23919/URSI-AT-RASC.2018.8471367, 2018.

Karia, S.P., Kim, J., Afolayan, A.O., and Lin, T.I.: A study on Nighttime Winter Anomaly (NWA) and other related Mid-latitude Summer Nighttime Anomaly (MSNA) in the light of International Reference Ionosphere (IRI) – Model, Adv. Space Res., 63, 6, 1949-1960, https://doi.org/10.1016/j.asr.2018.11.021, 2019.

Krankowski, A., Shagimuratov, I.I., Ephishov, I.I., Krypiak-Gregorczyk, A., and Yakimova, G.: The occurrence of the mid-latitude ionospheric trough in GPS-TEC measurements, Adv. Space Res., 43, 11, 1721-1731, https://doi.org/10.1016/j.asr.2008.05.014, 2009.

Lean, J.L., Meier, R.R., Picone, J.M., Sassi, F., Emmert, J.T., and Richards, P.G.: Ionospheric total electron content: Spatial patterns of variability, J. Geophys. Res. Space Phys., 121, 10,367–10,402, doi:10.1002/2016JA023210, 2016.

Lee, C.K., Han, S.C., Bilitza, D., and Chung, J.-K.: Validation of international reference ionosphere models using in situ measurements from GRACE K-band ranging system and CHAMP planar Langmuir probe, J. Geod., 85, 921-929, https://doi.org/10.1007/s00190-011-0442-6, 2011.

Matyjasiak, B., Przepiórka, D. and Rothkaehl, H.: Seasonal Variations of Mid-Latitude Ionospheric Trough Structure Observed with DEMETER and COSMIC, Acta Geophys., 64, 2734-2747, https://doi.org/10.1515/acgeo-2016-0102, 2016.

Mendillo, M., Huang, C.-L., Pi, X., Rishbeth, H., and Meier, R.: The global ionospheric asymmetry in total electron content, J. Atmos. Sol.-Terr. Phys., 67, 1377-1387, DOI: 10.1016/j.jastp.2005.06.021, 2005.

Rishbeth, H., Muller-Wodarg, I.C.F.: Why is there more ionosphere in January than in July? The annual asymmetry in the F2-layer, Ann. Geophys., 24, 3293-3311, DOI: 10.5194/angeo-24-3293-2006, 2006.

https://doi.org/10.5194/angeo-2019-124
Preprint. Discussion started: 18 September 2019

Annales Geophysicae Discussions

Rocken, C., Kuo, Y.H., Schreiner, W.S., Hunt, D., Sokolovskiy, S., and McCormick, C.: COSMIC System Description, Special issue of TAO (Terrestrial, Atmospheric and Oceanic Science), 11, 1, 21-52, DOI: 10.3319/TAO.2000.11.1.21(COSMIC), 2000.

Roma-Dollase, D., Hernandez-Pajares, M., Krankowski, A., Kotulak, K., Ghoddousi-Fard, R., Yuan, Y., Li, Z., Zhang, H., Shi, C., Wang, C., Feltens, J., Vergados, P., Komjathy, A., Schaer, S., Garcia-Rigo, A., and Gomez-Cama, J.M.: Consistency of seven different GNSS global ionospheric mapping techniques during one solar cycle, J. Geod., 92, 6, 691--706, 10.1007/s00190-017-1088-9, 2018.

Shepherd, S. G.: Altitude-adjusted corrected geomagnetic coordinates: Definition and functional approximations, J. Geophys. Res., 119, 9, doi:10.1002/2014JA020264, 2014.

Sun, Y.Y., Liu, J.Y., Tsai, H.F., and Krankowski, A.: Global ionosphere map constructed by using total electron content from ground-based GNSS receiver and FORMOSAT-3/COSMIC GPS occultation experiment, GPS Solution, 21, 1583-1591, https://doi.org/10.1007/s10291-017-0635-4, 2017.

Yasyukevich, Yu.V., Yasyukevich, A.S., Ratovsky, K.G., Klimenko, M.V., Klimenko, V.V., and Chirik, N.V.: Winter anomaly in NmF2 and TEC: when and where it can occur, J. Space Weather Space Clim., 8, A45, https://doi.org/10.1051/swsc/2018036, 2018.

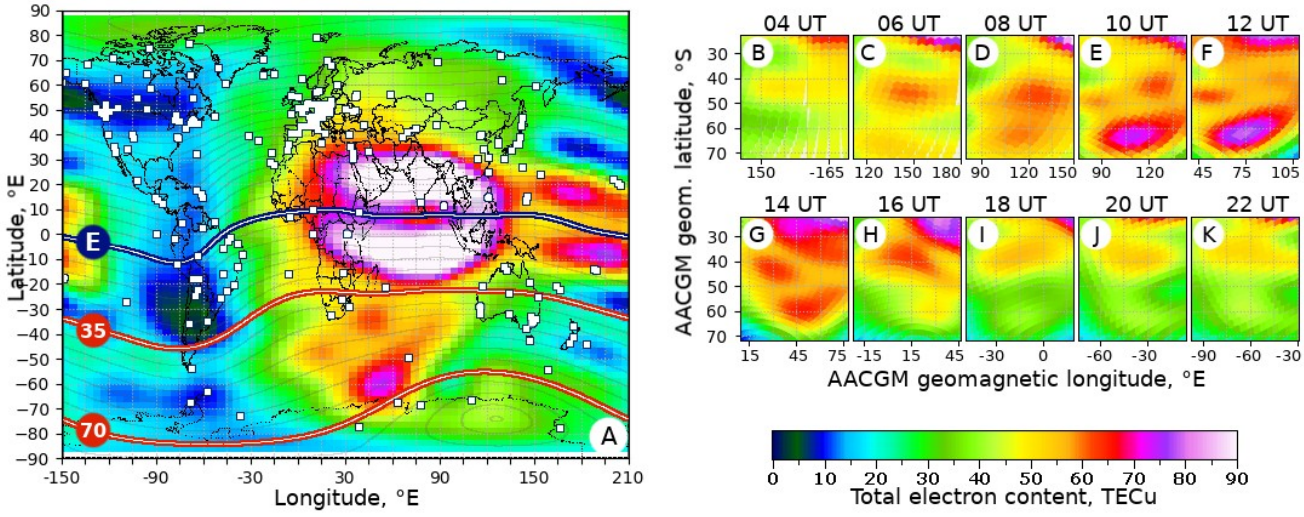

Figure 1: Intense LTE observed at 10:00 UT of 05.04.2014 near Antarctica (A) and its development during a day in geomagnetic coordinates (B-K). LTE develops along geomagnetic parallels in a region 35-70°S (A, red lines)

https://doi.org/10.5194/angeo-2019-124
Preprint. Discussion started: 18 September 2019

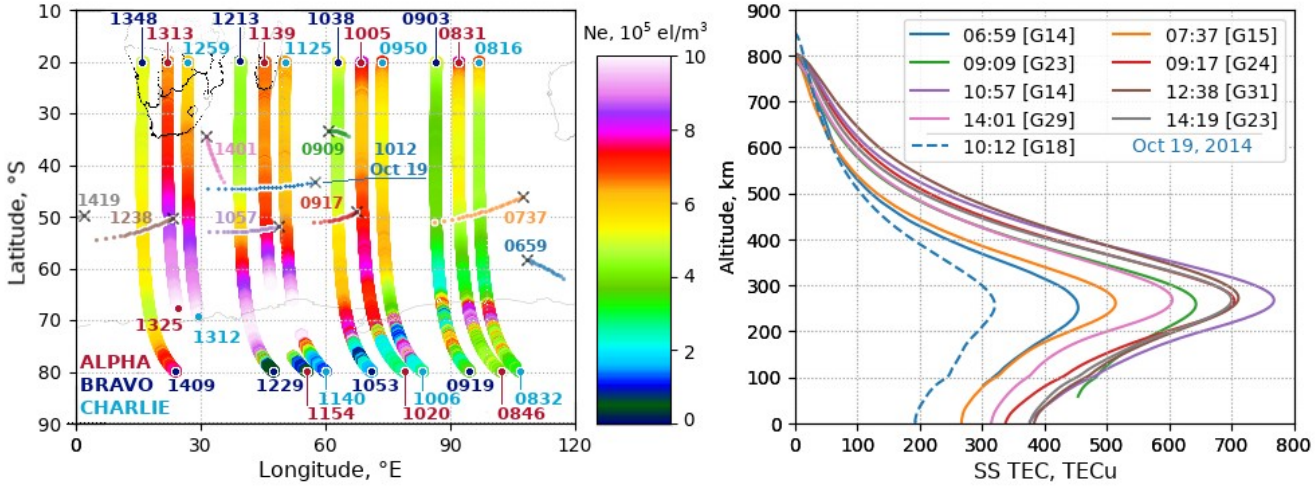

315 **Figure 2: Electron concentration during 8-14 UT of April 5, 2014 measured by SWARM (left) and total electron content from RO measurements by COSMIC satellites (right, solid). Compare with the profile of October 19, 2014 when no LTE was detected (right, dashed). Digits marks time of observation in a format HHMM (hours and minutes)**

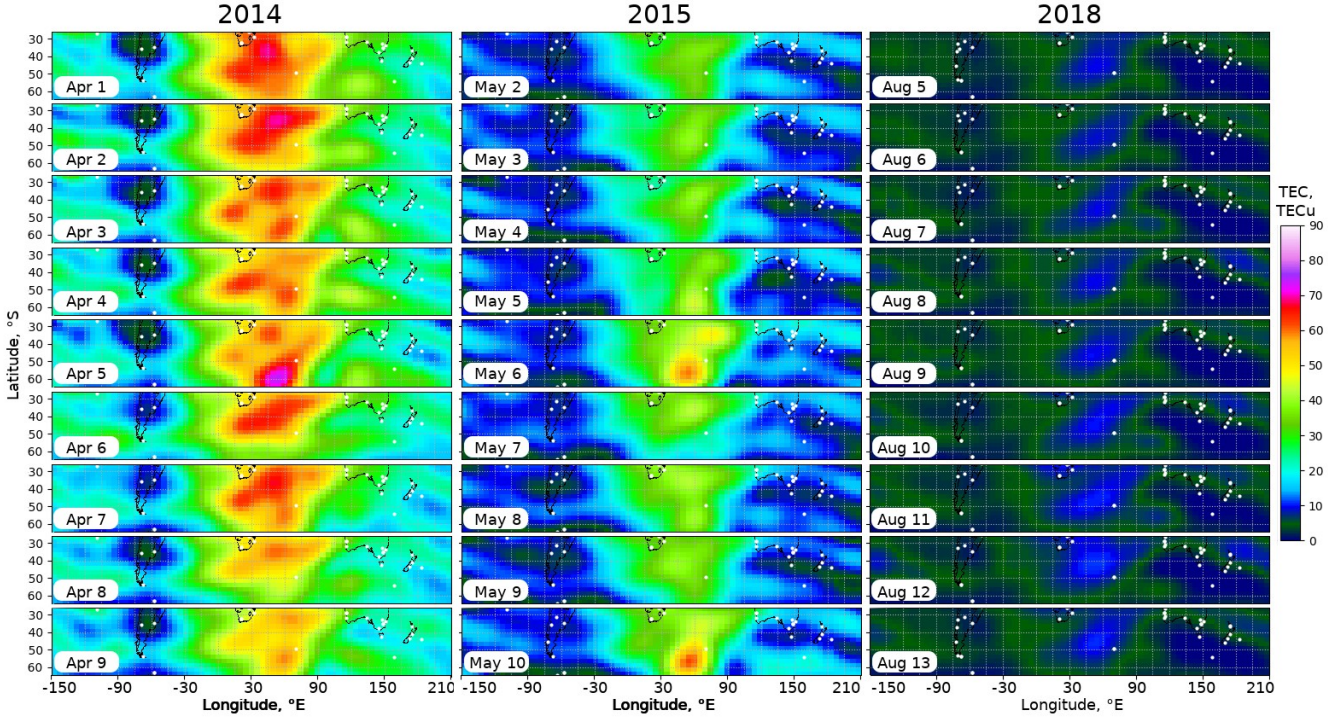

320 **Figure 3: Series of LTEs observed in Southern Hemisphere at 10 UT during years of different solar activity**

https://doi.org/10.5194/angeo-2019-124
Preprint. Discussion started: 18 September 2019

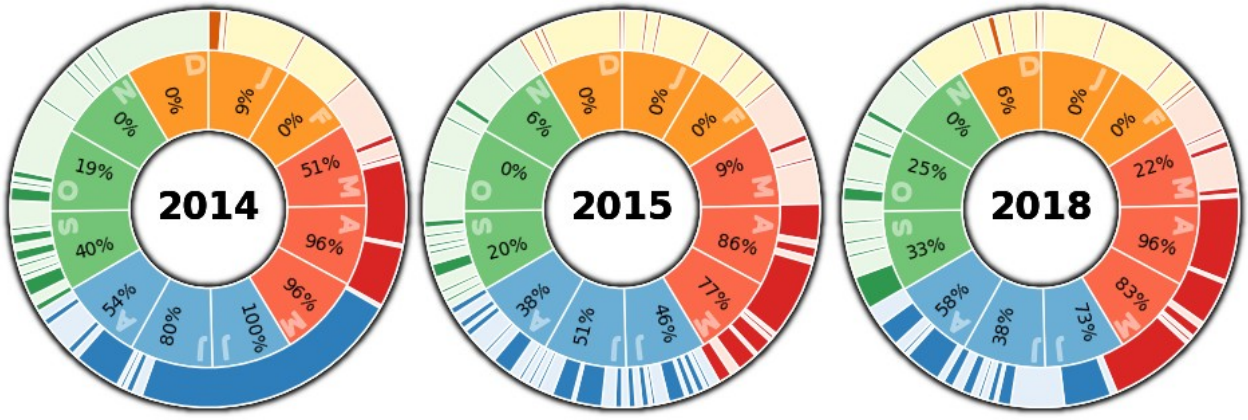

Figure 4: Percentage of days with series of LTEs observed during each year (inner sectors) and temporal position of each LTE (solid color) alternating with days without LTE (light color) (outer sector)

325

https://doi.org/10.5194/angeo-2019-124
Preprint. Discussion started: 18 September 2019

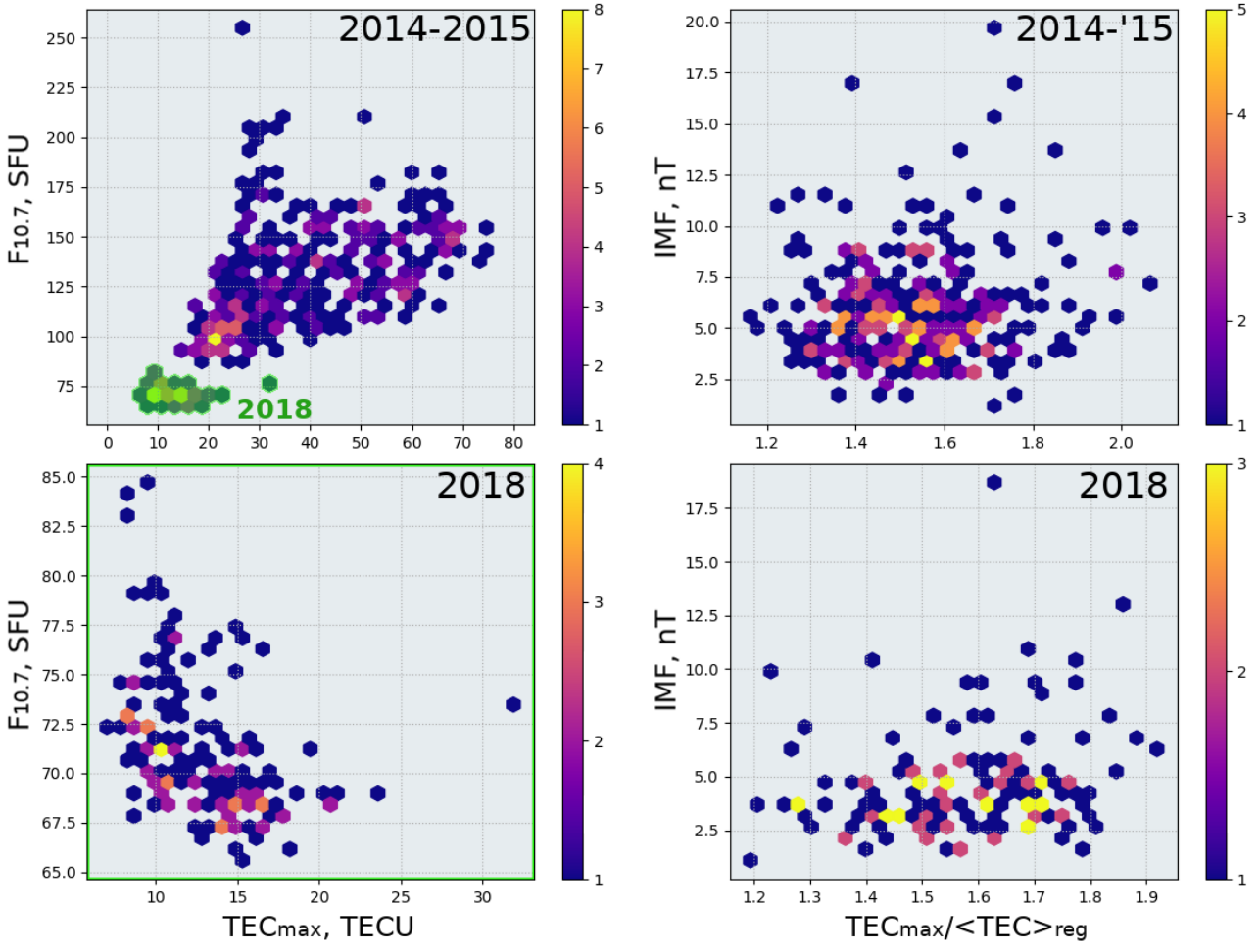

Figure 5: Distribution of maximal TEC values in a region 30°W-60°E, 30-60°S versus 10.7 nm solar radiation (left) and distribution of maximal to regional mean TEC ratio versus intensity of IMF (right). All the TEC values are taken for 10 UT separately during 2014-2015 (top) and 2018 (bottom). Color shows amount of LTEs detected in the corresponding conditions. Green-colored part (top, left) shows distribution for 2018